Catalytically active, magnetically separable, and water-soluble FePt nanoparticles modified with cyclodextrin for aqueous hydrogenation reactions

Kohsuke Mori,[a] Naoki Yoshioka,[a] Yuichi Kondo,[a] Tetsuya Takeuchi[b] and Hiromi Yamashita*[a]

Received 16th March 2009, Accepted 26th May 2009
First published as an Advance Article on the web 16th June 2009
DOI: 10.1039/b905331j

A new multifunctional FePt nanoparticle (NP) exhibiting catalytic activity, magnetic properties, and water-compatibility, has been developed. The initial thermal decomposition of iron carbonyl ($Fe(CO)_5$), followed by reduction of platinum acetylacetonate ($Pt(acac)_2$) in the presence of oleic acid and oleylamine produced FePt NPs with Fe-rich core and Pt-rich shell. The hydrophobic NPs were subsequently treated with γ-cyclodextrin (γ-CD), which renders them water-dispersible rather than in organic solvents. Characterization by means of X-ray diffraction (XRD), transmission electron microscopy (TEM), superconducting quantum interface device (SQUID), and X-ray absorption fine structure (XAFS) measurements were performed. The FePt NPs capped with γ-CD (FePt-γ-CD) had a mean diameter of *ca.* 2.5 nm, which exhibited superparamagnetic behavior at 300 K with zero remanence and coercivity. The FePt-γ-CD was successfully employed as an efficient nanocatalyst for the aqueous hydrogenation reactions with the easy recovering from the reaction mixture by applying an external magnet. Moreover, the FePt-γ-CD prefers the hydrogenation of allyl alcohol over sterically hindered 3-cyclohexene-1-methanol in the competitive reaction due to the molecular recognition property imposed by the surface attached γ-CD.

Introduction

The fabrication of nanoparticle (NP)-based materials have attracted much attention owing to their promising applications in optoelectronic, electronic, and catalysis that originate from the quantum size effects as well as large surface areas.[1] In the nanometre size regime, the physical and chemical properties become significantly dependent on their primary structures such as size, shape, crystal structure, composition, and protective ligand.[2] The synthetic methods providing suitable nanocrystals for any purpose are extremely important. Although NP-based catalysts possessing extremely large surface areas are key components of catalytic activity,[3] the separation step becomes a more troublesome issue. In order to overcome the above drawbacks, catalytic NPs have been stabilized by capping with ligands ranging from small organic molecules to large polymers or encapsulated within zeolite and mesostructured materials.[4] Alternatively, the separation of suspended magnetic NP catalysts from the liquid system using an external magnetic field is a promising strategy.[5] There have been some developments in the use of magnetic NPs to host soluble catalytically active organometallic complexes and enzymes;[6] however, the use of NP itself as catalytically active species is scarcely explored.

The synthesis of CD (cyclodextrin)-stabilized metal NPs represents research on the functionalization of NPs such as gold,[7] palladium,[8] and platinum.[9] CDs are a group of cyclic oligosaccharides composed of six (α-CD), seven (β-CD), or eight (γ-CD) α(1,4)-linked glucopyranose units. The cavity exhibits a hydrophobic character, which allows CDs to form inclusion complexes with hydrophobic molecules that fit into the cavity. Furthermore, such systems possess properties of the two components, in particular, the electronic, magnetic, or catalytic properties of the metal/semiconductor core and the molecular recognition ability of the receptors in the organic shell. This host–guest interaction may be applicable to drug delivery, chromatography, solubility enhancement, and selective removal of undesired substances.[10]

Herein, we present a CD-stabilized FePt magnetic NP exhibiting catalytic activity under aqueous conditions. The FePt NP was synthesized by the thermal decomposition of iron carbonyl ($Fe(CO)_5$) and subsequent reduction of platinum acetylacetonate ($Pt(acac)_2$) in the presence of oleic acid and oleylamine with the aim of producing a Fe-rich core and Pt-rich shell, which allows for the application to the Pt-based catalytic reactions. Oleic acid and oleylamine act as ligands to protect NPs against oxidation and aggregation, which are responsible for hydrophobicity and make them soluble in only nonpolar solvents. Such NPs have been transferred into aqueous solution through the formation of inclusion complexes between surface-bound molecules and cyclodextrins (Fig. 1), which successfully promote the environmentally-benign aqueous hydrogenation reactions. The present $Fe_{core}Pt_{shell}$ NP possess another attractive

[a]*Division of Materials and Manufacturing Science, Graduate School of Engineering, Osaka University, 2-1 Yamada-oka, Suita, Osaka, 565-0871, Japan. E-mail: yamashita@mat.eng.osaka-u.ac.jp; Fax: +81 6-6879-7457; Tel: +81 6-6879-7457*
[b]*Low Temperature Center, Osaka University, Japan*

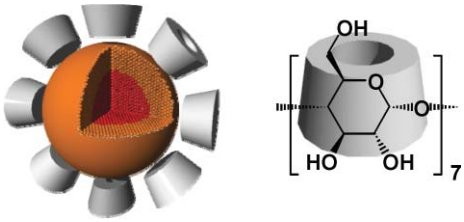

Fig. 1 Schematic illustration of FePt NP and γ-CD. The red core is Fe rich and the orange shell is Pt rich.

features compared to the single Pt component-based systems: Firstly, the replacement of the interior of precious Pt NPs with inexpensive core metals contribute to the atomic economy. Secondly, the magnetic core provides an opportunity for achieving the convenient separation of nanocatalyst after catalytic reaction by applying an external magnet. This study represents the first step in the possible application of CD-stabilized FePt NPs as a novel aqueous nanocatalyst.

Results and discussion

Fcc FePt NPs are commonly synthesized *via* co-reduction of an iron salt and platinum acethylacetonate, $Pt(acac)_2$ in the presence of oleic acid and oleylamine, which act as ligands to stabilize FePt NPs.[11] For the structural model of as-synthesized common FePt NPs, it is reasonable to suggest that most of the Pt atoms are preferentially located in the core region, while the Fe atoms are preferentially located in the shell region. Since the reduction potentials of Pt ions are more positive than Fe ions ($E°(Pt^{2+}/Pt°) = +1.2$ V, $E°(Fe^{2+}/Fe°) = -0.44$ V *vs.* NHE), the former are reduced first and constitute the core. This is followed by the reduction of Fe ions on the surface of the Pt core. However, such $Fe_{shell}Pt_{core}$ NPs are thought to be inappropriate for the application to the Pt-based catalytic reactions.

With this in mind, we controlled the composition of FePt NPs to form $Fe_{core}Pt_{shell}$ by applying successive reduction of metal precursors as follows. At first, $Fe(CO)_5$ was mixed with dibenzyl ether and the mixture heated to 523 K under Ar with vigorous mechanical stirring to form Fe core. Next, $Pt(acac)_2$, oleic acid, and oleylamine were then injected with mechanical stirring, and then the reaction mixture was heated at a rate of ~5 K/min to 583 K and kept stirring for 1 h. The resulting NPs were precipitated with excess ethanol and collected by centrifugation. As shown in Fig. 2a, the as-synthesized FePt NPs dispersed in nonpolar solvents such as hexane and toluene due to the presence of oleic acid and oleylamine.[10] Elemental analysis confirmed that the average composition of the NPs was $Fe_{48}Pt_{52}$.

To explore the possibility to stabilize catalytically active metallic NPs in water, the modification with γ-CD was performed. The mixture of hexane suspension of as-synthesized FePt NPs and equal volume of γ-CD aqueous solution was stirred vigorously at room temperature. After stirring for 24 h, the top hexane layer becomes colorless, confirming the existence of water-compatible γ-CD as host molecules (Fig. 2b). It can be said that the surface properties of the NPs have been modified through the formation of an inclusion complex between surface-bound organic molecules and γ-CD. The surface coverage of γ-CD on the FePt NPs is roughly estimated to be *ca.* 60% by

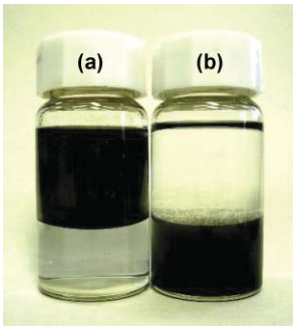

Fig. 2 Photograph of two-phase mixture of FePt NPs stabilized by oleic acid/oleylamine and (b) γ-CD. The top layer was hexane and bottom layer was aqueous solution.

CHN elemental analysis. In the FT-IR spectrum, the peaks due to the antisymmetric glycosidic ν_a(C–O–C) vibration and the coupled ν(C–C/C–C) stretch vibration were observed at 1028 and 1197 cm^{-1}, respectively. These NP are expected to be a single magnetic domain and exhibit a magnetic moment only in the presence of a magnetic field, indicating a superparamagnetic nature. When the magnetic field is removed, the particles immediately return to their nonmagnetic state.

In the XRD pattern of the FePt NPs stabilized with γ-CD, the intensities of the diffraction peaks are low, presumably due to the smaller size of the particles (Fig. 3). However, they exhibited clear peaks due to the fcc FePt around 40.0°, 46.7°, and 68.2°, corresponding to the (111), (200), and (220) reflections, respectively. Assuming that the FePt NPs are spherical in shape, the average crystalline size after encapsulation was calculated to be 2.9 nm by applying Scherrer's equation for the (111) reflection.

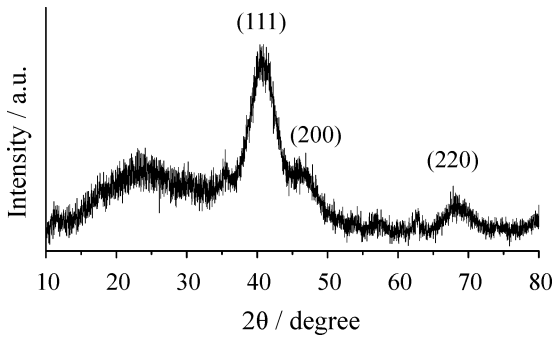

Fig. 3 XRD pattern of as-synthesized FePt NPs stabilized by γ-CD.

Fig. 4a and 4b shows a transmission electron microscopy (TEM) image and size distribution diagram. The FePt NPs having average diameter (d_{ave}) of *ca.* 2.5 nm were found to be distributed within the image area. The diffraction patterns exhibited atomic lattice fringes corresponding to the (111), (200), (220), and (113) planes of the fcc structure of the FePt NPs, respectively (Fig. 4c). This observation is consistent with the results of XRD analysis, as described earlier, verifying the single-crystalline nature of the particles.

The magnetic properties were investigated using a superconducting quantum interface device (SQUID) magnetometer (Fig. 5). The isothermal magnetization curve at 300 K displayed a rapid increase with increasing applied magnetic field, due to superparamagnetic relaxation.[12] This indicates that the thermal

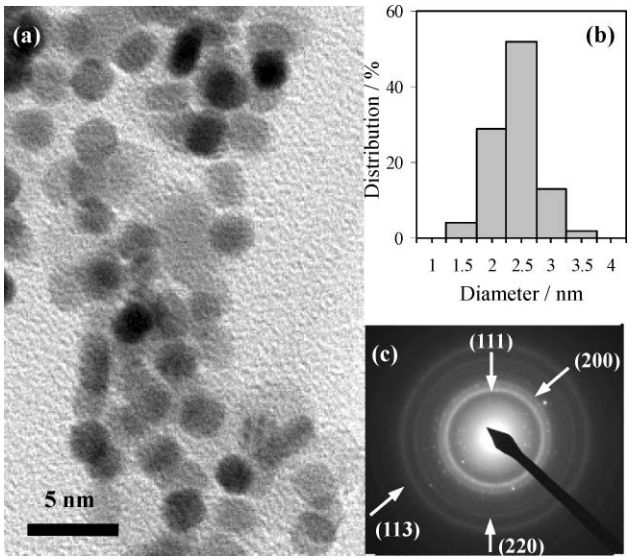

Fig. 4 TEM image, (b) size distribution diagram, and (c) electron diffraction pattern of FePt NPs stabilized by γ-CD.

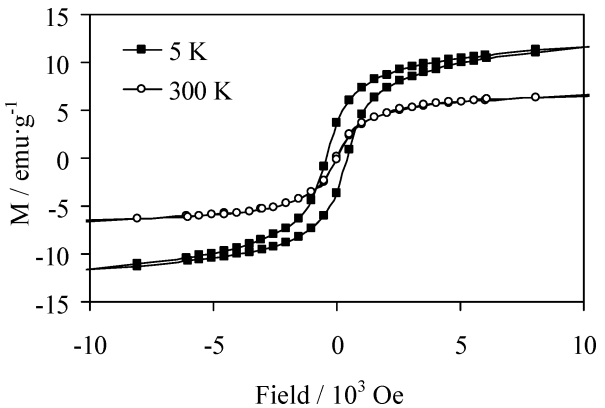

Fig. 5 Field-dependent magnetization curve for FePt NPs stabilized by γ-CD measured at 300 K (■) and 5 K (○).

energy can overcome the anisotropy energy barrier of the individual particles, and the net magnetization of these nanoparticle assemblies is zero in the absence of an external field. Hysteresis was absent with zero remanence (M_r) and coercivity (H_c), and the saturation magnetization (M_s) reached up to 12.5 emu/g. With decreasing temperature, the magnetization of both samples increased and exhibited a symmetric hysteresis loop at 5 K (M_r = 3.7 emu/g, H_c = 400 Oe), indicating a transition from superparamagnetic to ferromagnetic behavior.

X-ray absorption measurement was carried out to elucidate the electronic structure and chemical environment of the $Fe_{core}Pt_{shell}$ NPs stabilized by γ-CD in comparison to the $Fe_{shll}Pt_{core}$ NPs prepared by conventional co-reduction method. Fig. 6A shows the normalized X-ray absorption near-edge structure (XANES) spectra at the Pt L_{III}-edge of FePt NPs as well as standard samples including Pt foil and PtO_2. The white line at the Pt L_{III}-edge is an absorption threshold resonance attributed to the electronic transitions from $2p_{3/2}$ to unoccupied states above the Fermi level and is intensified with an increase in the *d*-band vacancies as a result of oxidation.[13] Therefore, the white line absorption peaks of PtO_2 at 11565 eV showed a

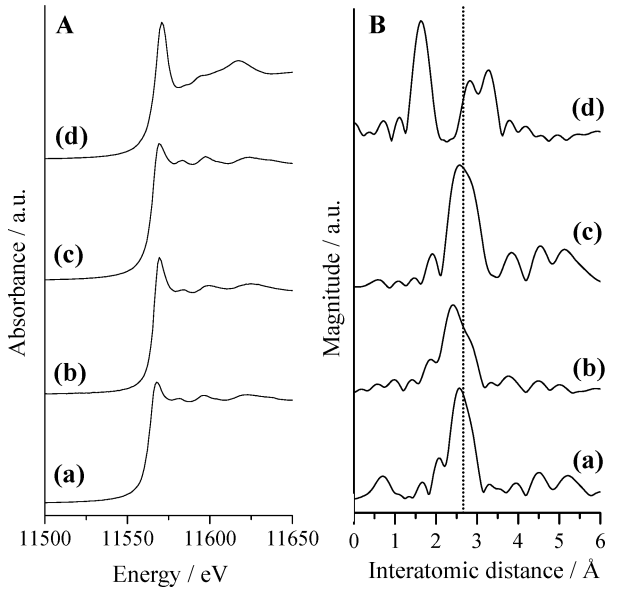

Fig. 6 **(A)** Pt L_{III}-edge XANES spectra and **(B)** FT-EXAFS spectra for $Fe_{shell}Pt_{core}$ NPs stabilized by γ-CD, (b) $Fe_{core}Pt_{shell}$ NPs stabilized by γ-CD, (c) Pt foil, and (d) PtO_2.

higher intensity. On the other hand, FePt samples and Pt foil afforded lower intensified peaks at 11563 eV, suggesting that the oxidation state of Pt in the FePt samples remained Pt^0. More detailed inspection revealed that the white line absorption peak of the $Fe_{core}Pt_{shell}$ NPs slightly higher than that of the $Fe_{shell}Pt_{core}$ NPs sample, indicating that Pt atoms in the shell region exist in a slightly higher oxidation state than that in the core region (**a** *vs.* **b**) due to the exposure to the surface. Fig. 6B shows the Fourier transforms (FT) of Pt L_{III}-edge extended X-ray absorption fine structure (EXAFS) spectra of these samples. FePt samples exhibited a single peak at approximately 2.4 Å, which could be assigned to the contiguous Pt–Pt bond in the metallic form. The Pt–Pt distance in $Fe_{core}Pt_{shell}$ sample, however, was found to be shorter than those of the pure Pt metal and $Fe_{shell}Pt_{core}$ NPs (2.7 Å), suggesting the presence of Fe–Pt heteroatomic bonding.[14] No peaks due to Pt–O and Pt–O–Pt bonds, detectable in that of Pt oxide at around 1.6 and 3.0 Å, were observed.

Fig. 7A shows the Fe K-edge XANES spectra of the FePt NPs and reference iron compounds. The edge position (measured at the half-height of the edge jump) depends on the electronic charge of the iron ion, and the energy increased in the order of Fe foil (7117.1 eV) < $Fe_{core}Pt_{shell}$ NPs (7118.0 eV) < $Fe_{shell}Pt_{core}$ NPs (7119.0 eV) < Fe_2O_3 (7122.0 eV). Thus, the iron elements in the $Fe_{shell}Pt_{core}$ NPs are more oxidized than those of the $Fe_{core}Pt_{shell}$ NPs because of the exposure to the surface. The FT-EXAFS spectra of the FePt samples demonstrated a peak between 1.5 and 2.9 Å, corresponding to the Fe–O and Fe–O–Fe bonds, accompanied with a slight peak at around 2.1 Å corresponding to the Fe–Fe bond (Fig. 7B). Compared to the Fe_2O_3 and $Fe_{shell}Pt_{core}$ NPs, the intensity of the second peaks for the $Fe_{core}Pt_{shell}$ NPs is significantly weakened. This peak is attributable to the contiguous Fe–O–Fe bonds due to face-, edge-, vertex-sharing FeO_6 octahedra. The reduced intensity of the $Fe_{core}Pt_{shell}$ NPs in this region can be explained by the structural disorder in the extremely small nanoparticles.[15] The iron oxide

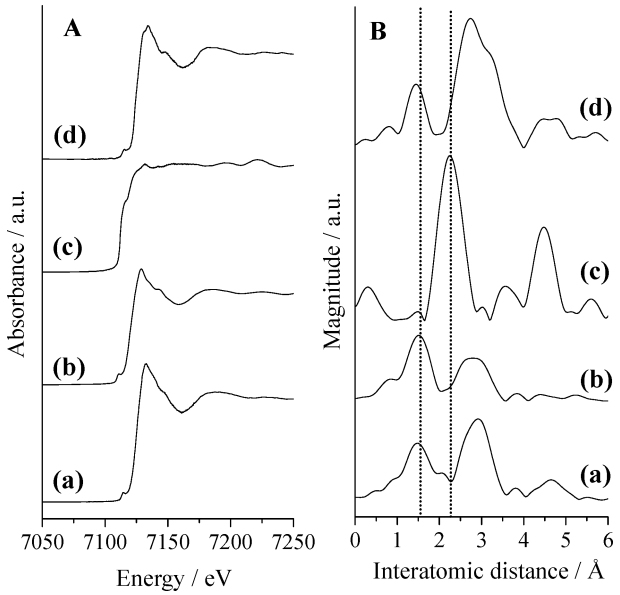

Fig. 7 **(A)** Fe K-edge XANES spectra and (**B**) FT-EXAFS spectra for $Fe_{shell}Pt_{core}$ NPs stabilized by γ-CD, (b) $Fe_{core}Pt_{shell}$ NPs stabilized by γ-CD, (c) Fe foil, and (d) Fe_2O_3.

particles in the core region are responsible for the weakness of high order coordination shell. For the structural model of the $Fe_{core}Pt_{shell}$ NPs, the overall results suggest that most of the Pt atoms are preferentially located in the shell region, the Fe atoms are preferentially located in the core region. The above speculation was supported by the catalytic results, as will be discussed later.

The use of water as a reaction medium instead of organic solvents has become increasingly frequent and specialized over the past few years.[16] Unique reactivity and selectivity that cannot be achieved under dry conditions are often observed in aqueous reactions due to the hydrophilic and hydrogen-bonding properties of water, even when solid catalysts are employed. Conducting reactions under aqueous conditions also provides the advantages such as reduced pollution, low cost, and simplicity in process and handling. The catalytic properties of the $Fe_{core}Pt_{shell}$ NPs capped with γ-CD were evaluated in the hydrogenation reaction of allyl alcohol in water under 1 atm of molecular hydrogen (Fig. 8). For comparison, catalytic experiments with $Fe_{core}Pt_{shell}$ NPs stabilized by oleic acid/oleylamine in water, $Fe_{core}Pt_{shell}$ NPs stabilized by oleic acid/oleylamine in THF, $Fe_{shell}Pt_{core}$ NPs stabilized by γ-CD, which was prepared by the conventional co-reduction method, in water were also performed. The aqueous reaction of allyl alcohol using $Fe_{core}Pt_{shell}$ NPs capped with γ-CD proceeded smoothly to give the corresponding *n*-propanol. It should be noted that the reaction using the $Fe_{shell}Pt_{core}$ NPs as well as Fe NPs stabilized by γ-CD hardly occurred because Fe atoms do not accelerate the above hydrogenation reaction, confirming that our FePt NPs consist of Fe-rich core and Pt-rich shell. More interestingly, the reaction rate performed with FePt NPs capped with γ-CD in water is three times higher than hydrophobic FePt NPs stabilized by oleic acid/oleylamine in THF. Similar results were observed in other organic solvents, such as toluene and hexane. We suppose that the host–guest complexation of organic substrate (allyl alcohol) with γ-CD on FePt NPs was

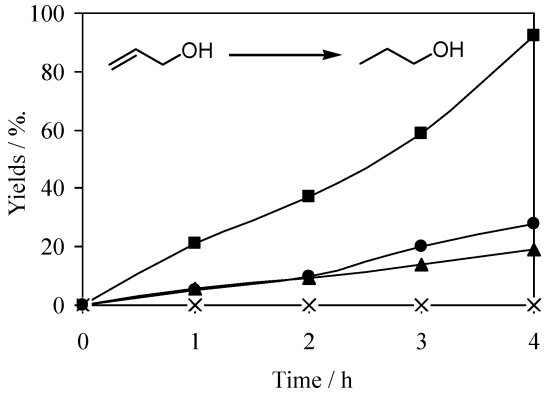

Fig. 8 Hydrogenation of allylic alcohol using $Fe_{core}Pt_{shell}$ NPs stabilized by γ-CD in water (■), $Fe_{core}Pt_{shell}$ NPs stabilized by oleic acid/oleylamine in water (●), $Fe_{core}Pt_{shell}$ NPs stabilized by oleic acid/oleylamine in THF (▲), $Fe_{shell}Pt_{core}$ NPs stabilized by γ-CD in water (×).

the major driving force for the enhancement of the catalytic efficiency under aqueous conditions. Such driving force was lost in the case of the hydrophobic FePt NPs stabilized by oleic acid/oleylamine in an organic solvent as the reaction medium, resulting in a low catalytic activity. The present catalytic system was also applicable to the reduction of *p*-nitrophenol, giving the corresponding *p*-aminophenol quantitatively (Scheme 1). An important advantage of the FePt NPs with γ-CD is the facile recovery from the reaction mixture and the high reusability. Upon completion of the reaction, the magnetic properties of the NPs can afford a straightforward means to isolate from the colloidal solution. By applying an external permanent magnet, the NPs were attracted. TEM analysis confirms that the size distribution of the recovered FePt NPs remained virtually unchanged. Moreover, the recovered FePt NPs with γ-CD could then be recycled at least three times while maintaining identical inherent activity to the initial run.

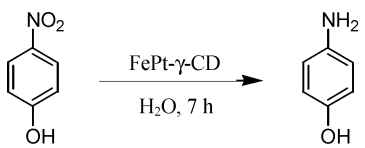

Conv. > 99 %

Scheme 1 Reduction of *p*-nitrophenol using H_2.

More significantly, in the hydrogenation of an equimolar mixture of allyl alcohol and 3-cyclohexene-1-methanol under aqueous conditions, the Pt/SiO_2 catalyst gave a product ratio of 5 for *n*-propanol and cyclohexanemethanol. On the other hand, the FePt NPs with γ-CD showed a high product ratio of 10 in which cyclohexanemethanol was obtained in 10% yield at a complete consumption of allyl alcohol (Scheme 2). It is assumed that the hydrogenation of sterically hindered 3-cyclohexene-1-methanol was inhibited by the molecular recognition properties imposed by the surface attached γ-CD. Our designed architecture enabled the powerful combination of useful functionality, magnetic property that was attracted to a magnetic field and a catalytically active site that exhibited prominent activity and selectivity for aqueous catalytic reactions.

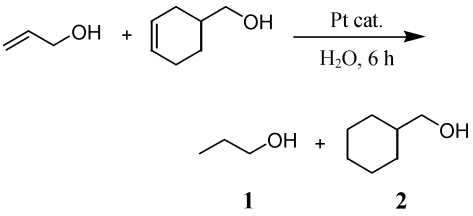

	Product ratio (**1**/**2**)
FePt-γ-CD	10
Pt/SiO_2	5

Scheme 2 Competitive hydrogenation of allyl alcohol and 3-cyclohexene-1-methanol.

Conclusion

The first example of the catalytic application under aqueous conditions using magnetic FePt NPs was presented. The dispersity of the as-synthesized FePt NPs stabilized by oleic acid and oleylamine in water was drastically improved by the formation of an inclusion complex between surface-bound organic molecules and γ-CD. Characterization by several physicochemical methods revealed that superparamagnetic fcc FePt NPs with an average diameter of 2.5 nm. Most of the Pt atoms are preferentially located in the shell region, while the Fe atoms are preferentially located in the core region. The resulting FePt NPs showed an enhanced catalytic activity in water rather than in organic solvents and host–guest recognition properties to facilitate the reaction of sterically less hindered substrate was also observed.

Experimental section

The synthesis of $Fe_{core}Pt_{shell}$ NPs

FePt NPs were prepared using a Schlenk line by airless techniques. Iron pentacarbonyl (1.0 mmol, $Fe(CO)_5$, Aldrich) was mixed with 100 mL of dibenzyl ether (Tokyo Kasei Kogyo Co., Ltd) in a 500 mL three-neck flask. The mixture was degassed for 1 h and then heated to 523 K under Ar with vigorous mechanical stirring for 10 min. Platinum acetylacetonate (0.5 mmol, $Pt(acac)_2$, Wako Pure Chemical Ind., Ltd.), 1 mmol of oleic acid (Wako Pure Chemical Ind., Ltd.), and 1 mmol of oleylamine (Aldrich) were then injected with mechanical stirring. The reaction mixture was heated at a rate of ~5 K/min to 583 K and maintained for 1 h. The black colored solution was allowed to cool to room temperature and NPs were precipitated with excess ethanol and collected by centrifugation. After washing several times with toluene, ethanol, and distilled water, the precipitate was uniformly dispersed in hexane.

The synthesis of $Fe_{shell}Pt_{core}$ NPs

$Fe(CO)_5$ (1.0 mmol) and $Pt(acac)_2$ (0.5 mmol) were mixed with 100 mL of dibenzyl ether in a 500 mL three-neck flask. The mixture was degassed for 1 h and then heated to 523 K under Ar with vigorous mechanical stirring. Oleic acid (1 mmol) and oleylamine (1 mmol) were then injected with mechanical stirring. The reaction mixture was heated at a rate of ~5 K/min to 583 K and maintained for 1 h. The black colored solution was allowed to cool to room temperature and NPs were precipitated with excess ethanol and collected by centrifugation. After washing several times with toluene, ethanol, and distilled water, the precipitate was uniformly dispersed in hexane.

The modification procedure of the FePt NPs with γ-CD

The modification was conducted by vigorous stirring of the mixture of hexane suspension of FePt NPs and equal volume of γ-CD (Aldrich) aqueous solution at room temperature. The concentration of NPs in hexanes was ~0.5 mg particle/mL, and the concentration of γ-CD aqueous solution was 10 mM. After stirring for 24 h, the top hexane layer become colorless, and was discarded; while the bottom aqueous layer was collected. After washing several times with water, the precipitate was stored in water.

Characterization

X-ray diffraction patterns were recorded using a Rigaku Miniflex using Cu Kα radiation of wavelength 1.5418 Å. Elemental analysis was performed with EDX-720 (Shimadzu). Infrared spectra were obtained with a JASCO FTIR-6100. Samples were diluted with KBr and compressed into thin disk-shaped pellets. TEM micrographs were obtained with a Hitachi Hf-2000 FE-TEM equipped with a Kevex energy-dispersive X-ray detector operated at 200 kV. The magnetic properties were measured with a Quantum Design MPMS-XL. Fe K-edge and Pt L_{III}-edge XAFS spectra were recorded at room temperature in fluorescence mode at the BL-7C and BL-9A facilities at the Photon Factory at the National Laboratory for High-Energy Physics, Tsukuba (2007G031, 2007G077). A Si(111) double crystal was used to monochromatize the X-rays from the 2.5 GeV electron storage ring. In a typical experiment, the sample was loaded into the *in situ* cell with plastic windows. The EXAFS data were examined using an EXAFS analysis program, Rigaku EXAFS. The pre-edge peaks in the XANES regions were normalized for atomic absorption, based on the average absorption coefficient of the spectral region. Fourier transformation (FT) of k^3-weighted normalized EXAFS data was performed over the 3.0 Å $< k/Å^{-1} <$ 12 Å range for Fe K-edge sample and 3.5 Å $< k/Å^{-1} <$ 12 Å range for Pt L_{III}-edge sample to obtain the radial structure function.

Typical examples for the aqueous hydrogenation

Into a reaction vessel (50 mL) with a reflux condenser were placed catalyst (3 mg), allyl alcohol (2.0 mmol), and distilled water (10 ml). The resulting mixture was reacted at 293 K for 4 h under 1 atm of H_2 with magnetic stirring. Analytical GC was performed using a Shimadzu GC-14B with flame ionization detector equipped with polar pack Q column. Yield was determined by the following equation: yield = [area of product]/[area of substrate + area of product]. The hydrogenation of *p*-nitrophenol was conducted by the similar method with catalyst (3 mg), *p*-nitrophenol (1.0 mmol), and distilled water (10 ml). The resulting mixture was reacted at 293 K for 7 h under 1 atm

of H_2. Part of the mixture was taken out after every 10 min and centrifuged for the determination with UV photospectrometer.

Acknowledgements

This work was supported by Priority Assistance for the Formation of Worldwide Renowned Centers of Research—The Global COE Program (Project: Center of Excellence for Advanced Structural and Functional Materials Design) from the Ministry of Education, Culture, Sports, Science and Technology (MEXT), Japan. The authors appreciate Dr Eiji Taguchi and Prof. Hirotaro Mori at the Research Center for Ultra-High Voltage Electron Microscopy, Osaka University for assistance with TEM measurements. X-ray adsorption experiments were performed at the Photon Factory of KEK (2007G031, 2007G077).

References

1 (*a*) J. P. Wilcoxon and B. L. Abrams, *Chem. Rev.*, 2006, **35**, 1162; (*b*) J. D. MacKenzie and E. P. Bescher, *Acc. Chem. Res.*, 2007, **40**, 810; (*c*) S. G. Kwon and T. Hyeon, *Acc. Chem. Res.*, 2008, **41**, 1696.
2 D. L. Laslie-Pelecky and R. D. Rieke, *Chem. Mater.*, 1996, **8**, 1770.
3 (*a*) M. A. El-Sayed, *Acc. Chem. Res.*, 2001, **34**, 257; (*b*) D. Astruc, F. Lu and J. R. Aranzaes, *Angew. Chem. Int. Ed.*, 2005, **44**, 7852.
4 (*a*) M. Arai, Y. Takada and Y. Nishiyama, *J. Phys. Chem. B*, 1998, **102**, 1968; (*b*) M. Zhao and R. M. Crooks, *Angew. Chem. Int. Ed.*, 1999, **38**, 364; (*c*) J. W. Yoo, D. Hathcock and M. A. El-Sayed, *J. Phys. Chem. A*, 2002, **106**, 2049; (*d*) P. Concepción, A. Corma, J. Silvestre-Albero, V. Franco and J. Y. Chane-Ching, *J. Am. Chem. Soc.*, 2004, **126**, 5523; (*e*) K. Mori, T. Hara, T. Mizugaki, K. Ebitani and K. Kaneda, *J. Am. Chem. Soc.*, 2004, **126**, 10657.
5 (*a*) K. Mori, S. Kanai, T. Hara, T. Mizugaki, K. Ebitani, K. Jitsukawa and K. Kaneda, *Chem. Mater.*, 2007, **19**, 1249; (*b*) K. Mori, Y. Kondo, S. Morimoto and H. Yamashita, *Chem. Lett.*, 2007, **36**, 1068; (*c*) K. Mori, Y. Kondo, S. Morimoto and H. Yamashita, *J. Phys. Chem. C*, 2008, **112**, 2593; K. Mori, K. Sugihara, Y. Kondo, T. Takeuchi, S. Morimoto and H. Yamashita, *J. Phys. Chem. C*, 2008, **112**, 16478.
6 (*a*) M. T. Reetz, A. Zonta, V. Vijayakrishnan and K. Schimossek, *J. Mol. Catal. A*, 1998, **134**, 251; (*b*) X. Gao, K. M. K. Yu, K. Tam and S. C. Tsang, *Chem. Commun.*, 2003, 2998; (*c*) H. M. R. Garadimalla, D. Mandal, P. D. Stevens, M. Yen and Y. Gao, *Chem. Commun.*, 2005, 4432; (*d*) P. D. Stevens, G. Li, J. Fan, M. Yen and Y. Gao, *Chem. Commun.*, 2005, 4435; (*e*) V. Polshettiwar and R. S. Varma, *Chem. Eur. J.*, 2009, **15**, 1582; (*f*) V. Polshettiwar and R. S. Varma, *Org. Biomol. Chem.*, 2009, **7**, 37; (*g*) V. Polshettiwar, B. Baruwati and R. S. Varma, *Chem. Commun.*, 2009, 1837; (*h*) V. Polshettiwar, B. Baruwati and R. S. Varma, *Green Chem.*, 2009, **11**, 127.
7 (*a*) J. Liu, W. Ong, E. RomÁn, M. J. Lynn and A. E. Kaifer, *Langmuir*, 2000, **16**, 3000; (*b*) J. Liu, J. Alvarez and A. E. Kaifer, *Adv. Mater.*, 2000, **12**, 1381; (*c*) Y. Liu, K. B. Male, P. Bouvrette and J. H. T. Luong, *Chem. Mater.*, 2003, **15**, 4172.
8 J. Alvarez, J. Liu, E. Roman and A. E. Kaifer, *Chem. Commun.*, 2000, 1151.
9 S. Giuffrida, G. Ventimiglia, S. Petralia, S. Conoci and S. Sortino, *Inorg. Chem.*, 2006, **45**, 508.
10 (*a*) S. O. Fakayode, M. Lowry, K. A. Fletcher, X. Huang, A. M. Powe and I. M. Warner, *Curr. Anal. Chem.*, 2007, **3**, 171; N. Funasaki, S. Ishikawa and S. Neya, *Pure Appl. Chem.*, 2008, **80**, 1511.
11 (*a*) S. Sun, C. B. Murray, D. Weller, L. Folks and A. Moser, *Science*, 2000, **287**, 1989; (*b*) E. Shevchenko, D. Talapin, A. Kornowski, J. Kotzler, M. Haase, A. Rogach and H. Weller, *Adv. Mater.*, 2002, **12**, 287; (*c*) B. Jeyadevan, A. Hobo, K. Urakawa, C. N. Chinnasamy, K. Shinoda and K. Tohji, *J. Appl. Phys.*, 2003, **93**, 7574; (*d*) M. Nakaya, Y. Tsuchiya, K. Ito, Y. Oumi, T. Sano and T. Teranishi, *Chem. Lett.*, 2004, **33**, 130; (*e*) H. G. Bagaria, E. T. Ada, M. Shamsuzzoha, D. E. Nikles and D. T. Johnson, *Langmuir*, 2006, **22**, 7732; (*f*) V. Nandwana, K. E. Elkins, N. Poudyal, G. S. Chaubey, K. Yano and J. P. Liu, *J. Phys. Chem. C*, 2007, **111**, 4185.
12 J. M. Coey and D. Khalafalla, *Phys. Status. Solidi. A*, 1972, **11**, 229.
13 S. Feast, M. Englisch, A. Jentys and J. A. Lercher, *Appl. Catal. B: Environ.*, 1998, **174**, 155.
14 (*a*) K. Shinoda, K. Sato, B. Jeyadevan, K. Tohji and S. Suzuki, *J. Magn. Magn. Mater.*, 2007, **310**, 2387; (*b*) D.-Y. Wang, C.-H. Chen, H.-C. Yen, Y.-L. Lin, P.-Yu Huang, B.-J. Hwang and C.-C. Chen, *J. Am. Chem. Soc.*, 2007, **129**, 1538.
15 (*a*) S.-T. Wong, J.-F. Lee, S. Cheng and C.-Y. Mou, *Appl. Catal. A: General*, 2000, **198**, 115; (*b*) T. Liu, L. Guo, Y. Tao, T. D. Hu, Y. N. Xie and J. Xhang, *Nanostruct. Mat.*, 1999, **11**, 1329.
16 (*a*) C.-J. Li, and T.-H. Chan, Eds., *Organic Reactions in Aqueous Media*, WileyNew York, 1997; (*b*) S. Kobayashi and S. Manabe, *Acc. Chem. Res.*, 2002, **35**, 209.

